Original Research

Cucurbitacin B and cisplatin induce the cell death pathways in MB49 mouse bladder cancer model

Yener Kurman[1], Ilker Kilicciogl u[1,2], Asiye U Dikmen[3], Guldal Esendagli[4], Cenk Y Bilen[5], Sinan Sozen[6] and Ece Konac[1]

[1]Department of Medical Biology and Genetics, Faculty of Medicine, Gazi University, Ankara 06510, Turkey; [2]Department of Medical Biology, Faculty of Medicine, Duzce University, Duzce 81620, Turkey; [3]Department of Public Health, Faculty of Medicine, Gazi University, Ankara 06510, Turkey; [4]Department of Pathology, Faculty of Medicine, Gazi University, Ankara 06510, Turkey; [5]Department of Urology, Faculty of Medicine, Hacettepe University, Ankara 06100, Turkey; [6]Department of Urology, Faculty of Medicine, Gazi University, Ankara 06510, Turkey

Corresponding author: Ece Konac. Email: ecemercanoglu@yahoo.com

Impact statement

Alternative agents that will increase the effectiveness of cisplatin, which are widely used in the advanced stage and metastatic bladder cancer, are being investigated. In previous studies, Cucurbitacin B (CuB), which is a natural compound from the Cucurbitaceae family has been shown to inhibit the proliferation of tumor cells and create synergistic effects with cisplatin. In this study, we investigated the synergistic effect of CuB with cisplatin for the first time in bladder cancer *in vitro* and *in vivo* models. Our findings showed that CuB treatment with cisplatin reduced cell proliferation, and reduced tumor development through activating apoptosis and autophagy via PI3K/AKT/mTOR signaling pathway. Our results showed that CuB may be a new agent that can support conventional treatment in bladder cancer. Our study is important in terms of enlightening new pathways and developing new treatment methods in the treatment of bladder cancer.

Abstract

Cisplatin-based chemotherapy is the standard regimen for bladder cancer patients, but its effectiveness is limited by high toxicity and the development of drug resistance. It has been reported in many studies that Cucurbitacin B has anti-carcinogenic effects by stimulating apoptosis and autophagy. Here we explored the potential role of cucurbitacin B on MB49 bladder syngeneic mouse tumor model. Single and combined doses of cucurbitacin B and cisplatin were applied to MB49 cell line and the cell viability was determined by Water-Soluble Tetrazolium Salt-1 (WST) method. After developing the tumor model, mice were randomly divided into four groups and then cucurbitacin B and cisplatin applied in the specified doses and time. The expression levels of apoptosis (Bcl-2, Bax, Caspase-3, cleaved Caspase-3) and autophagy proteins (Beclin-1 and LC3I, LC3II) were detected by Western Blot. Phospho-protein array analysis was performed to determine the relative levels of phosphorylation of proteins which are associated with the PI3K-Akt signaling pathway. Tumor tissues were analyzed by hematoxylin-eosin staining. In the present study, the results showed that cucurbitacin B inhibited the expression of Bcl-2 and increased the expression of Bax and cleaved Caspase 3. LC3II is markedly up-regulated in cucurbitacin B-treated cells. Cucurbitacin B reduced the phosphorylation of p27, PRAS40, and Raf-1 proteins. CuB + Cis combination synergistically decreased phosphorylation of AKT, ERK1/ERK2, mTOR, BAD levels and increased the level of AMPKα. PI3K/AKT/ mTOR pathway might be one of the targets of cucurbitacin B in MB49 bladder cancer mouse model. CuB + Cis combination reduced the tumor growth. Cucurbitacin B has no toxic effects on lung, liver, kidney, heart, and bladder. Indeed, cucurbitacin B can inhibit the tumor proliferation; induce caspase-dependent/-independent apoptosis and autophagy. Our study provided a novel perspective to research the effects of cucurbitacin B on the apoptotic and autophagic pathways in bladder cancer and a new target class for drug development.

Keywords: Bladder cancer, cucurbitacin B, apoptotic proteins, autophagic proteins, syngeneic mouse models, combination therapy

***Experimental Biology and Medicine* 2020; 245: 805–814. DOI: 10.1177/1535370220917367**

Introduction

Bladder cancer is a malignancy that is responsible for a significant proportion of cancer deaths around the world. According to the Global Cancer Statistics 2018 data,[1] 549,000 new bladder cancer cases and 200,000 deaths are expected worldwide. Combined treatments involving cisplatin (Cis) have been used effectively for many years as first-line therapy in the treatment of advanced and metastatic bladder cancers. Although, cisplatin is of vital importance in the treatment of metastatic bladder cancer, response rate to cisplatin-based treatments is about 50% and the disease recurs in the majority of individuals receiving this treatment.[2] Also, frequent development of drug resistance and toxicity reduces clinical administration and effectiveness of cisplatin.[3,4] While drug combinations do increase the efficacy of treatment by reducing the harmful effects, their administration is subject to further research.[4,5]

Cucurbitacins are a group of tetracyclic triterpenoids that are widely isolated from the Cucurbitaceae plant family. These natural compounds have been used as a traditional treatment for centuries due to their anti-inflammatory, anti-microbial, anti-diabetic, and anti-cancer properties. They are separated into 12 groups due to diversity in their molecular composition.[6,7] Among these, terpenoid cucurbitacin B (CuB) is the most studied type owing to its anti-tumor effects in *in vitro* and *in vivo* studies.[5–9] Some of these studies have shown that CuB arrests cell cycle at certain stages according to the type of cancer cells and activates the cell death pathways.[5,7–10] CuB has been shown to induce apoptosis via Bcl-2 family proteins (decreased anti-apoptotic Bcl-2 and increased pro-apoptotic Bax) by inhibiting the CIP2A/PP2A/Akt; JAK2/STAT3 and MAPK pathways.[8,11–13] In some cancer cell lines it has been shown that reactive oxygen species produced by CuB causes DNA damage and autophagy.[14–16] It has also been reported that CuB activates autophagy by the mammalian target of rapamycin complex 1 (mTORC1) inhibition in the cisplatin-resistant gastric cancer cell line.[17] Combined administration of CuB and cisplatin has been shown to increase the effectiveness of cisplatin by creating a synergistic effect in various tumor models.[5–8,11,12] In these tumor models, it was shown that combined applications increase cell proliferation inhibition, cell cycle arrest, and apoptosis more effectively than individual applications.[6–8] Although apoptosis is the main cause of death from chemotherapy, autophagic cell death is another significant cause of death. Autophagy may result in either cell survival or cell death. This situation depends on the type of cancer, the genetic background of cancer cells or the external stress conditions to which the cells are exposed. Beclin-1, which is a member of the Class III PI3K complex, plays a role in the formation of double autophagosome membranes.[18] While microtubule-associated protein light chain 3–I (LC3-I) is dispersed in the cytoplasm, lipid-added LC3 (LC3-II) begins to accumulate in newly formed autophagosome membranes and is used as a marker for monitoring autophagy.[19]

To date, there are not any studies performed to investigate the effects of CuB-only or CuB + Cis combination treatment on bladder cancer. We aim to investigate the effects of CuB and Cis combined treatment targeting protein expression levels of apoptotic pathway proteins—Bcl-2, Bax, Caspase-3, Cleaved (Cl) Caspase-3- and autophagy pathway proteins—Beclin-1 and LC3I, LC3II—on MB49 bladder syngeneic mouse tumor model. In addition, we aimed to unveil the reason why CuB-only or CuB + Cis combination-treated tumor cells are prone to apoptosis or autophagy by analyzing the phosphorylated profiles of phosphatidylinositol 3-kinase (PI3K)/AKT signaling pathway.

Materials and methods

Reagents and antibodies

We studied with CuB (98% purity) and Cis (95% purity) purchased from Cayman (Ann Arbor, MC, USA). Both agents were dissolved in dimethyl sulfoxide (DMSO) and stock concentrations were prepared at 18 mM and 33 mM respectively and then stored at −20°C up to utilization. Fetal bovine serum (FBS), penicillin–streptomycin, phosphate-buffered solution (PBS), and 0.25% trypsin were bought from Biological Industries (Cromwell, CT, USA). Antibodies to Bcl-2, Bax, Beclin-1, β-actin were bought from Bioassay Technology Laboratory (Shanghai, China); Caspase-3, Cl Caspase-3, LC3I, and LC3II were bought from Cell Signaling Technology (Beverly, MA, USA). Horseradish Peroxidase (HRP)-conjugated goat anti-rabbit IgG was bought from Bioassay Technology Laboratory (Shanghai, China).

Cell line and cell culture

MB49 cell line was kindly provided by Dr. Güneş Esendağlı (Hacettepe University, Cancer Institute, Department of Basic Oncology). MB49 cells were cultured with RPMI-1640 medium supplemented with L-glutamine, 10% FBS, 100 U/mL penicillin, and 100 mg/mL streptomycin in an incubator providing humidified atmosphere with 5% CO_2 at 37°C.

Cell viability assay

Water-Soluble Tetrazolium Salt-1 (WST-1) kit (Sigma-Aldrich St. Louis, USA) was used to assess the cell viability. Cultured cells were seeded into each well (4×10^4 cells) of a 96-well plate with 100 µL of culture medium and incubated overnight in a humidified environment with 5% CO_2 and at 37°C to adhere cells on the well surface before CuB-only, Cis-only, and CuB + Cis combination treatment. The next day, after removing the media from the cells, various doses of CuB (0.01–50 µm) and Cis (0.5–50 µm) were implemented to cells for 24 h and 48 h; 10 µL of WST-1 reagent was then added to the wells and incubated at 37°C for 2 h. With the completion of the incubation, optical density in each well was detected using a microplate ELISA reader (SpectraMax M3, Molecular Devices, Silicon Valley, California, USA) at a wavelength of 440 nm.

Syngeneic mouse bladder tumor model

To establish a syngeneic mouse bladder tumor model, 1×10^6 MB49 cells in 100 µL cold PBS were injected subcutaneously into the right flank of the each C57BL/6 mouse strain. Mouse weights and tumor volumes were measured regularly three times in a week. Varnier caliper was used for tumor size measurement. Formula: (width × length × height) × 0.5 was referenced in the calculation of tumor size. When the tumor volumes reached a diameter of approximately 5 mm, mice were randomly divided into four groups (total *n*: 40; each group consists of 10 animals) and CuB and Cis applications started: (1) DMSO diluted with PBS was injected intraperitoneally to treated control; (2) Cis (3 mg/kg) was administered to Cis treatment group by intraperitoneal injection twice weekly; (3) CuB (1 mg/kg) was administered to CuB treatment group by intraperitoneal injection three times per week; (4) Cis (2 mg/kg) was injected intraperitoneally twice a week and CuB (0.5 mg/kg) was injected intraperitoneally three times a week to the combined treatment group.

In the light of the literature data,[20] we determined the optimal administration dose of CuB alone as 1 mg/kg. Researchers working with CuB previously stated that this concentration of the drug and the frequency of administration were safe for mice. In our study, we determined the dose as 3 mg/kg for Cis. Considering the literature, cisplatin applications are available in higher concentrations.[21,22.] However, our aim here was to prevent cisplatin-induced toxicity. This dose is based on previous studies on lethal dose 50 (LD50) values for cisplatin. In combined dose applications, we reduced the dose of both drugs so that we can prevent drug-induced internal organ toxicity and reduce the tumor volume synergistically.

Two days after the last administration, treatment was terminated on the 19th day. At the end of treatment, animals were euthanized under deep anesthesia by taking intra-cardiac blood. A portion of the tumor tissues were stored at –80°C for further molecular analysis. The remaining tissues (lung, liver, heart, kidney, and bladder) were kept in 10% formaldehyde for histological analysis. The animal experiments were approved by the Animal Experiments Local Ethics Committee of Gazi University (G.Ü.ET-18.028).

Histopathological examination

Tumor and possible metastasis tissues—lung, liver, kidney, heart and bladder—were excised from animals and fixed in 10% formaldehyde. Fixed samples were embedded in paraffin blocks. These paraffin blocks were cut into 4 µm by using a rotary microtome and stained with routine hematoxylin-eosin (H&E) dyes and examined histopathologically under light microscope. Histopathological examination mainly focused on both primary tumor sites metastasis and toxic effects of the CuB-only, Cis-only, and CuB + Cis treatments on the aforementioned five tissues.

Western blot analysis

Radioimmunoprecipitation assay (RIPA) buffer containing protease inhibitor was used for protein isolation from tumor tissues. The concentration of isolated proteins was determined by the bicinchoninic acid (BCA) protein kit (Thermo Fisher Scientific Inc., Waltham, USA). Equal amounts of protein samples were mixed with 4× sample buffer and boiled in dry heater at 95°C for 5 min. After the boiling process, protein samples were loaded into 10–12% sodium dodecyl sulfate (SDS)-polyacrylamide gel and transferred to polyvinylidene difluoride (PVDF) membrane by using Bio-Rad transfer equipment (Bio-Rad, Hercules, CA, USA). Membranes were washed with Tris-buffered saline with 0.05% Tween-20 (TBST) and blocked with 5% BSA at room temperature for 1 h. The membrane was incubated overnight at 4°C with primary antibodies specific to the targeted proteins (dilution 1:1000) at +4°C and then incubated with HRP-conjugated secondary antibody (dilution 1:5000) at room temperature for 2 h. Membranes treated with ECL solution (Thermo Fisher Scientific, Waltham, MA, USA) were imaged by Gel Logic 2200 Pro imaging system (Carestream Health, Rochester, New York, USA). Numerical values of signal intensity were measured by image J program (NIH, Bethesda, Maryland, USA). β-actin antibody was used as the control gene for protein expression.

Protein phosphorylation membrane array

Human/Mouse AKT Pathway Phosphorylation Array C1 kit (Georgia, ABD) was used to investigate the change in phosphorylation of 18 proteins (p-Akt, p-AMPKα, p-BAD, p-ERK 1&p-ERK 2, p-GSK3a, p-GSK3b, p-mTOR, p-p27, p-p53, p-P70S6K, p-4E-BP1, p-PDK1, p-PRAS40, p-PTEN, p-Raf-1, p-RPS6, p-RSK1, p-RSK2) associated with the PI3K-Akt signaling pathway. Assay was performed according to the protocol given by the manufacturer. The amount of protein to be added to the membrane was determined by BCA method and sample volumes were adjusted to 3000 µg total protein amount. After the sample incubation overnight, the membranes were washed with solutions. After the washing step, a biotin-labeled antibody mixture was placed on the membranes and the membranes were incubated again overnight. The next day, HRP-anti-rabbit IgG mixture was added and allowed to incubate overnight. After incubation, the membranes were washed again and the samples on the membranes were determined by chemiluminescent irradiation in the presence of imaging solution as in the Western Blot method. Image J program was used for quantification.

Statistical analysis

The data obtained from the experimental results were analyzed using SPSS 21.0 statistical program. Results from each experiment were presented as mean ± standard deviation (SD) of three independent experiments. Kruskal–Wallis test was used to evaluate the difference between the group averages. Bonferroni-corrected ($P < 0.016$) Mann–Whitney U test was used for the comparison of pairs—CuB-only and

Cis-only; CuB-only and combined (CuB + Cis) group; Cis-only and combined (CuB + Cis) group—and between each group and control. $P < 0.05$ was accepted as statistically significant for comparisons among all groups in terms of evaluating cell viability.

Results

CuB reduced the viability of MB49 cells by generating a synergistic effect with cisplatin

To evaluate the effects of CuB and Cis, single and combined doses of these agents were administered to MB49 cells at different time intervals. The viability of MB49 cells decreased with increasing drug doses and administration time. CuB causes cell death at lower doses compared to Cis. The IC_{50} dosages for cisplatin were found 30 μM after 24 h of incubation and 20 μM after 48 h of incubation (Figure 1(a)). CuB inhibited the viability of MB49 cells in a concentration-dependent and time-dependent manner, and IC_{50} values for CuB after 24 h and 48 h were 0.5 μM and 0.25 μM, respectively (Figure 1(b)). IC_{50} values obtained after 24 h of co-administration of these two agents were 0.05 μM for CuB and 20 μM for Cis. Furthermore, IC_{50} values after 48 h were found 0.1 μM and 10 μM for CuB and Cis, respectively (Figure 1(c)). A significant decline was observed in IC_{50} values after combined treatments as opposed to single agent treatments (Figure 1(c)).

CuB+Cis combination reduced tumor growth in MB49 syngeneic mouse model

The effects of CuB and Cis on tumor development were evaluated in a bladder cancer syngeneic mouse model induced by MB49 cells. Tumor volumes and weights in single and combined treatment groups were significantly smaller compared to the control group (Figure 2(a) to (c)) ($P < 0.05$). Single administration of Cis and CuB as well as administration of the combined group significantly inhibited tumor growth (tumor volume averages are 52%, 62% and 77% respectively) (Figure 2(a)) ($P < 0.05$). Tumor weights indicated a correlation with tumor volumes and the minimum increase in mean tumor weights was seen in the combined group (Figure 2(b)) ($P < 0.05$). There was no significant change in body weights in the CuB-treated group and CuB treatment caused no toxic effects.

Histopathological findings

Tumor formation was observed in all groups before the treatment process. The largest tumor diameter and the

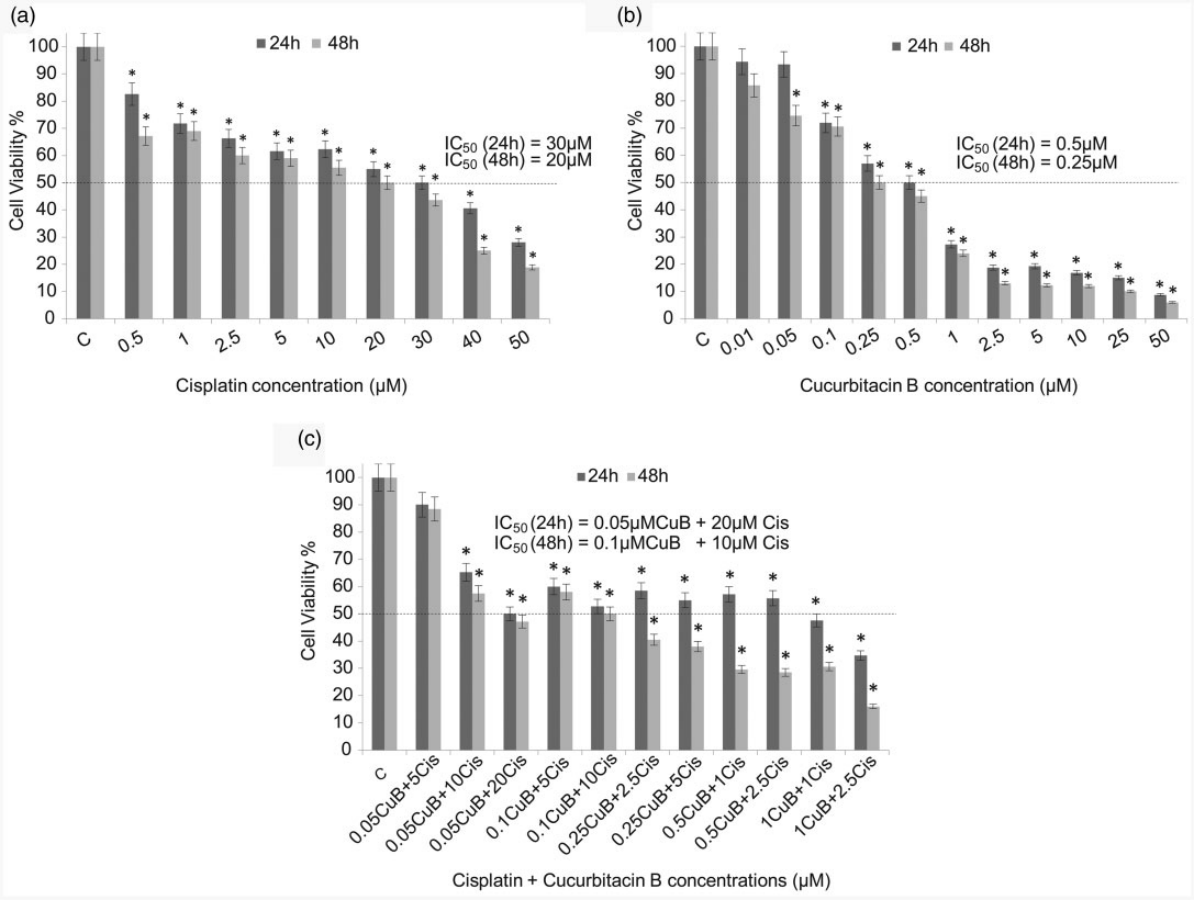

Figure 1. Effects on cell viability with single (a, b) and combined (c) doses of CuB and Cis on MB49 cell lines after 24 h and 48-h exposures. The IC_{50} values indicate a concentration of compounds which caused 50% reduction in cell viability based on WST-1 assay.
C: control; Cis: cisplatin; CuB: cucurbitacin B. *indicated $P < 0.05$, compared with the non-treated group. Data were presented as the means ± SD from three independent experiments in the histograms.

largest area of necrosis were found in the control group (Figure 2(d)). The smallest tumor development was monitored during the combined treatment. Tumor cells had large vesicular hyperchromatic nuclei, prominent nucleoli, and medium width cytoplasm. There were no differences in mitosis rates among the groups; 7–12 mitosis /1 high-power field (hpf) was observed in all groups.

Toxicity was evaluated according to the following features: In the liver, portal inflammation, globular inflammation, steatosis, Kupffer cells hyperplasia were evaluated. In the lung, inflammation, congestion, and hemorrhage were evaluated. In renal tissue, tubular necrosis, inflammation, and glomerular pathology were evaluated. Heart necrosis was also evaluated. Lung metastasis was detected in all groups. Although metastasis was observed in more than one lobe in the control group, an animal with the smallest tumor diameter was seen in the combined group (Figure 2 (e)). In the control group and in the treatment groups, no histopathological changes or metastasis were found in the liver, kidney, heart, and bladder sections. The histological features can be seen in Figure 2(d) and (e).

CuB induced cell apoptosis and autophagy in MB49 mouse tumor tissues

To investigate the effects of CuB and Cis on apoptotic pathway, expression levels of Bcl-2, Bax, Caspase-3, and Cl Caspase-3 were detected by the Western Blot method. Compared to the control group, anti-apoptotic Bcl-2 protein levels decreased significantly in the treatment groups (Figure 3(a) and (b)). The decrease in Bcl-2 expression was higher in the Cis group than in the CuB group, and statistically significant decreases were seen in all treated (Cis, CuB, CuB + Cis) groups (Figure 3(a) and (b)), while in groups treated with CuB-only and Cis-only, pro-apoptotic Bax protein expression levels increased about 3-folds;

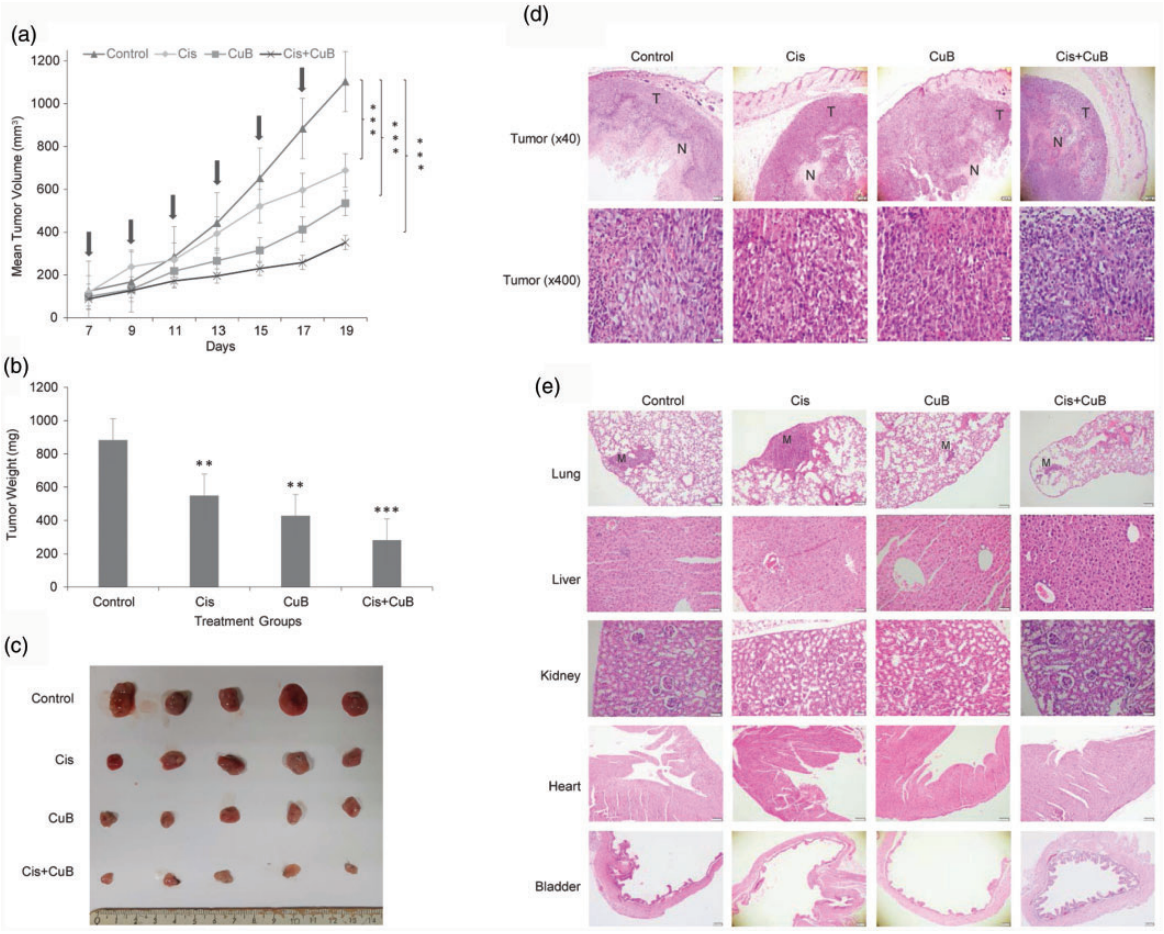

Figure 2. C57BL/6 mouse strain was injected subcutaneously with 1 × 106 MB49 cells in 100 μL PBS. After injection, tumor volumes were measured regularly with caliper. Tumor volumes were calculated according to the formula: (length×width×depth) × 0.5. Tumor-bearing mice were divided into four groups ($n = 10$ per group). Control group received phosphate-buffered saline (pbs) diluted DMSO. Treatment groups received; Cis (3 mg/kg), CuB (1 mg/kg), both Cis (2 mg/kg) and CuB (0.5mg/kg), respectively. Treatment started on day 7. Drug applications were made on the days indicated in the graph (Arrows indicated days of treatment). The last injection was performed on day 17 and two days later, on day 19, the mice were sacrificed, tumor tissues were removed, and their weight measured. (a) Tumor volumes were significantly reduced in the treatment groups when compared with the control group. (b) Mean weights of tumor tissues removed from mice in each group after treatment. (c) Representative images of tumors excised from control and single/or combined doses of CuB and Cis-treated MB49 bearing mice. (d and e) Hematoxylinand eosin staining of extracted tumor tissues and organs (lung, liver, kidney, heart, and bladder) after treatment. CuB and Cis administration did not cause any toxic effects on organs listed in the photo. Each bar represented the mean ± SD. ***$P < 0.001$, **$P < 0.01$, indicate statistically significant differences between pairs—CuB-only and Cis-only; CuB-only and combined (CuB + Cis) group; Cis-only and combined (CuB + Cis) group—and between each group and control. Cis: cisplatin; CuB: cucurbitacin B; T: tumor; N: necrosis; M: metastasis. (A color version of this figure is available in the online journal.)

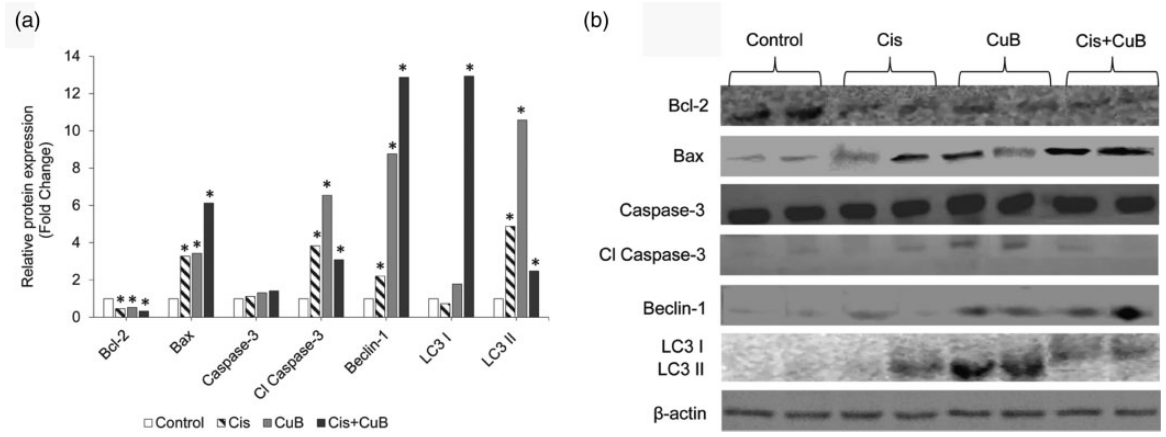

Figure 3. (a) Relative expression levels of apoptotic (Bcl-2, Bax, Caspase-3, and Cl Caspase-3) and autophagy proteins (Beclin-1, LC3I, LC3II) after CuB, Cis, and CuB+Cis treatment. (b) Western blotting analysis showing protein expression in CuB, Cis, and CuB+Cis treated-cells using the antibodies indicated. *$P < 0.05$ indicate statistically significant differences between pairs—CuB-only and Cis-only; CuB-only and combined (CuB+Cis) group; Cis-only and combined (CuB+Cis) group—and between each group and control. β-actin, also known as a "housekeeping" protein, was used as a loading control. β-actin: beta-actin; Cl Caspase-3: cleaved caspase-3; Cis: cisplatin; CuB: cucurbitacin B.

this increase was about 6-folds in the combined group (Figure 3(a) and (b)) ($P < 0.05$). On the other hand, there were not any significant differences in Caspase 3 levels in the treated groups. In all treated groups, the expression levels of Cl Caspase-3 were found significantly higher (Figure 3(a) and (b)) ($P < 0.05$). The maximum increase in the expression levels of Cl Caspase-3 was observed in the CuB-treated group (Figure 3(a) and (b)) ($P < 0.05$), suggesting that CuB might be assisting the initiation of apoptosis by triggering the mitochondrial apoptotic pathways.

To determine changes in autophagy pathway in tumor tissues, the expression levels of Beclin-1, LC3I, and LC3II were examined by the Western Blot method. While a statistically significant increase was found in the expression levels of Beclin-1 in Cis-only and CuB-only treated groups, the highest increase in Beclin-1 level was observed in the combined (CuB + Cis) group (Figure 3(a) and (b)) ($P < 0.0001$). In the combined treatment group, expression levels of Beclin-1 increased roughly 13-folds ($P < 0.0001$). LC3I protein expression level was found significantly higher in the combined treated groups when compared the single agent-treated groups (Figure 3(a) and (b)) ($P < 0.0001$). CuB significantly up-regulated the LC3II levels compared to the control group. However, a significant decrease was seen in the LC3II levels in the combined treatment group compared to the single agent-treated groups (Figure 3(a) and (b)). Cisplatin may have reduced the autophagic activity of CuB and perhaps the combined use of these two agents does not have a synergistic effect. According to our results, increased LC3II and Beclin-1 protein levels indicate that especially CuB stimulates the autophagy pathway.

CuB reduced the phosphorylation of p27, PRAS40, and raf-1 proteins

Cyclin-dependent kinase inhibitor 1B (p27Kip1) is a protein that regulates the cell cycle. Phosphorylation at thr198 affects the stabilization and activation of this protein. p27 phosphorylation at thr198 causes accumulation of this protein in the cytoplasm and progression of the cell cycle. In the CuB treatment group, the amount of phosphorylated p27 (p-p27) decreased significantly compared to the control group (Figure 4(a) and (b)) ($P < 0.05$). The proline-rich Akt substrate of 40 kDa (PRAS40) is the target protein of AKT. This protein is associated with PI3K/Akt and the mTOR pathways. Phosphorylation of PRAS40 increases the activation of these pathways. PRAS40 phosphorylation significantly decreased in the CuB treatment group when compared to the control groups (Figure 4(a) and (b)) ($P < 0.05$), while no significant change was observed in the other treatment groups. Raf-1 is a serine-threonine kinase that affects cell proliferation and death. Ser301 phosphorylation is associated with the active form of this protein. A statistically significant decrease in Raf-1 phosphorylation was observed in the CuB treatment group (Figure 4(a) and (b)) ($P < 0.05$).

CuB+cis combination synergistically decreased phosphorylation of AKT, ERK1/ERK2, mTOR, BAD levels and increased the level of AMPKα

AKT phosphorylation decreased in CuB and combined groups. In the combined group, phospho-AKT protein levels decreased to half of the amount in the control group (Figure 4(a) and (b)). Phospho-forms of extracellular signal-regulated kinase 1 (ERK1) (pT202/pY204) and ERK2 (pT185/pY187) decreased in all treatment groups; in particular, the amount of phosphorylation of the ERK1 protein significantly declined in the combined group. Phosphorylation levels of AMPKα increased in the single treatment groups but the highest increase was observed in the combined group (Figure 4(a) and (b)) ($P < 0.05$). While phosphorylation levels of mTOR protein decreased gradually in Cis and CuB groups, the significant decline was seen in the combined group (Figure 4(a) and (b)) ($P < 0.05$). Phosphorylation of BCL2-associated agonist of cell death (BAD) results in loss of ability of BAD to heterodimerize with the survival proteins BCL-X_L or BCL-2. This leaves Bcl-2 free to inhibit Bax-triggered apoptosis.

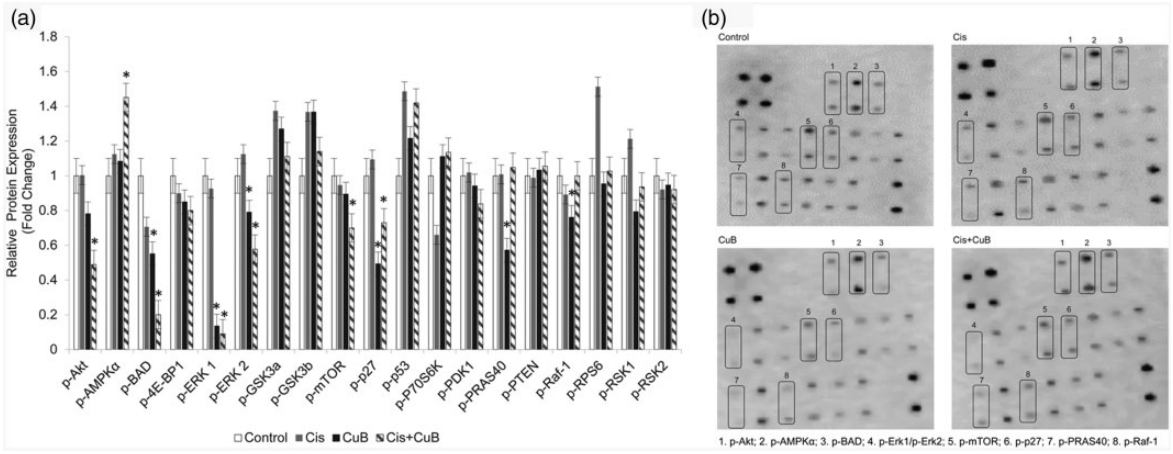

Figure 4. Phosphorylation levels of target proteins after CuB and Cis treatment was determined by Human/Mouse AKT Pathway Phosphorylation Array C1 kit. Four membrane arrays were used for control and treated groups. (a) Quantification of blot density levels of phospho-proteins from four membrane array were represented as bar graph with relative protein expression levels (b) Phospho-proteins array analysis with significant expression changes were indicated by numbered square frames. Phospho-proteins in numbered frames were listed. Blot densities were determined with image J program. Each bar represented the mean ± SD. $*P < 0.05$ indicate statistically significant differences between pairs—CuB-only and Cis-only; CuB-only and combined (CuB+Cis) group; Cis-only and combined (CuB+Cis) group—and between each group and control. Cis: cisplatin; CuB: cucurbitacin B.

Phosphorylation at Ser112 reduces the apoptotic activity of BAD protein; BAD phosphorylation thus is anti-apoptotic. We analyzed the expression levels of p-BAD by comparing a control group with treated groups. CuB and CuB + Cis combined groups showed a significant decrease (Figure 4 (a) and (b)) ($P < 0.05$). The decrease in the amount of phospho-BAD in the CuB group was higher than in the Cis group, while the maximum decline was seen in the combined group (Figure 4(a) and (b)) ($P < 0.05$).

Phosphorylation of other proteins–4E-BP1, GSK3a, GSK3b, P53, P70S6K, PDK1, PTEN, RPS6, RSK1, RSK2–remained unchanged in all treated groups (Figure 4(a) and (b)).

Discussion

In this study, we aimed to investigate the anti-cancer properties of CuB and its effect with Cis by evaluating protein expression changes in apoptotic and autophagic pathways. First, we demonstrated that CuB alone exhibits a strong anti-proliferative effect against bladder cancer. CuB inhibited cell proliferation at very low doses compared with Cis. In addition, it also enabled cisplatin to act at low concentrations. In other words, CuB produced a synergistic effect with Cis and increased its activity against cancer cell viability. This interaction allowed Cis to have the same effect at lower doses, so this effect may be important for reducing the high dose-induced toxic effects of Cis in clinical use. Second, single administration of CuB and administration in combination with Cis significantly inhibited tumor growth in bladder tumor tissues by stimulating apoptosis and autophagy pathways.

Anti-apoptotic Bcl-2 and pro-apoptotic Bax proteins belong to the Bcl-2 family and are the main regulators of the apoptotic pathway. Bcl-2 overexpression is associated with poor prognoses in bladder cancer and reduces the response of bladder cancer to chemotherapy.[23] Caspases are cytoplasmic proteases specific to the apoptotic pathway and execute apoptosis by digesting intracellular proteins. Cl Caspase-3 is the main executer of cell death and is responsible for the cutting of many proteins used as markers of apoptosis. According to our results, the increase in Bax and Cl Caspase 3 expression and the decrease in anti-apoptotic Bcl-2 expression showed that CuB and Cis induced the apoptotic pathway. The Western blot analysis in our study especially demonstrated that CuB inhibited the expression of Bcl-2 and increased the expression of Bax. These results are compatible with other studies showing that CuB induces apoptosis.[11,13] We found that in all treated groups the expression levels of Cl Caspase-3 were significantly higher ($P < 0.05$). The highest Cl Caspase-3 expression was seen in the CuB-treated group, but the same increasing rate was not seen in the CuB + Cis combine treatment group. These results suggest that CuB administration, whether on its own or together with Cis, induces apoptotic pathways in tumor tissues. When we look at the Cl Caspase 3 expression levels, we see that the application of CuB alone was more effective than the application of Cis alone. Therefore, the decrease in Cl Caspase 3 expression level in combined dose administration suggested that Cis may be less effective. However, tumor development was lower in the combined group when compared with other treated groups. These results suggest that the caspase-independent pathway and other cell death pathways, for instance, autophagy, might be active as well as the dependent pathway. The relationship between Bcl-2/Bax regulates apoptosis via the mitochondrial pathway in caspase-independent cell death, as in caspase-dependent cell death.[24] As in caspase-dependent cell death, Bax disrupts the mitochondrial membrane integrity and then ensures the release of pro-apoptotic proteins such as apoptosis-inducing factor (AIF) and Endo G from mitochondria to the cytoplasm. By the transition of these pro-apoptotic proteins into the nucleus, these proteins cause

caspase-independent death through DNA condensation and degradation. In fact, the two pathways may be activated simultaneously.[24,25]

Autophagy is a biological event in which cellular proteins and organelles are digested by lysosomal enzymes in autophagolysosomes in order to be re-used in subsequent reactions. Although autophagy is known to protect cells against various stress conditions, it is known that some drugs cause autophagic cell death by over-stimulating autophagy. Therefore, it is suggested that autophagy may be an alternative cell death pathway to be targeted in cancer treatment.[26] Recently, CuB induced autophagy in a human, cisplatin-resistant gastric cancer cell line.[17] In our study, we investigated the expression levels of Beclin-1, which take part in the initiation of autophagy and LC3II, accepted as a marker of autophagy. When cells underwent autophagy, LC3I with an 18-kDa molecular weight converted into 16-kDa LC3II. The amount of LC3II is closely correlated with the number of autophagosomes, serving as an indicator of autophagy.[27,28] According to our results, autophagy was induced in all treatment groups, and the expression level of LC3II was highest in the CuB group and lowest in the CuB + Cis group. Our results showed that autophagy was mostly induced in the CuB treatment group. Interestingly, levels of Beclin-1 expression were increased 13-fold in the combined group when compared with the control group. That is to say, the expression levels of Beclin-1 and LC3II are not correlated with each other. In the literature, there are some studies showing that autophagosome formation occurs independently of Beclin-1 function, known as non-canonical autophagy.[29,30] There is evidence that this type of autophagy is always associated with cell death.[30] Also, it was shown that Beclin-1 and LC3 expression are independent of each other in some cells in which autophagy occurs due to drug stimulation.[29–31] We found that CuB increased the level of LC3II protein expression significantly when compared to the Cis group. Although the LC3I protein expression level was highest in the combined group, LC3II expression did not accompany this increase. These results suggest that cisplatin may have reduced the autophagic activity of CuB. Furthermore, perhaps the combined use of these two agents has no synergistic effect in autophagy. Therefore, CuB could stimulate autophagy through different pathways in an MB49 mouse syngeneic bladder cancer model.

Stimulation and initial stages of autophagy are mainly regulated by the mammalian target of rapamycin (mTOR), AMP-activated protein kinase (AMPK), and AKT (Protein Kinase B).[32] AMPKα senses the low amount of energy in the cell and stimulates the transition to the catabolic process to produce ATP.[32] AMPKα also stimulates autophagy by inhibiting mTOR kinase.[32,33] Low AMPKα phosphorylation is also seen in bladder cancer.[34] AKT activates mTOR by phosphorylating it, and then activated mTOR suppresses autophagy. AKT kinase also inhibit autophagy by phosphorylating the components of the PI3K complex.[35] The effects of the three kinase (PI3K)/AKT/mTOR pathway on tumor development is well defined in bladder cancer, as in many other cancers.[35] With its stimulation by extracellular signals, this pathway controls cell proliferation, differentiation, and angiogenesis and plays a role in cancer formation. Approximately 40% of bladder tumors show mutations that cause continuous activation of this pathway.[35] An increase in the amount of phospho-mTOR (p-mTOR) has been demonstrated in the invasive forms of bladder cancer. In addition, p-mTOR density is associated with decreased survival in bladder cancer.[36] Consistent with other studies, we found that CuB + Cis treatment reduced p-mTOR and p-Akt levels and enhanced p-AMPK levels.[15–17,37] These results indicate that the PI3K/AKT/mTOR pathway is a target of CuB in the MB49 bladder cancer mouse model and that CuB-mediated autophagy may also be associated with this pathway.

BAD is a pro-apoptotic member of the BCL-2 family. It binds to the anti-apoptotic Bcl-2 protein, disrupts the Bcl-2/Bax complex, and allows Bax to induce apoptosis. Ser-112 phosphorylation of BAD prevents this protein from being retained in the cytoplasm by 14–3-3 protein and binding to BCL-2. Thus, ser-112 phosphorylation inhibits the pro-apoptotic effect of BAD.[38] The amount of phosphorylated BAD decreased in all treatment groups, especially in the combined group, in which a 5-fold reduction was observed. In particular, the decrease in BAD phosphorylation in the CuB and combined groups suggests that the apoptotic pathway was induced in these groups. It has previously been suggested that the phosphorylation of BAD at Ser-155 may convey oncogenic potential.[39] There are no other studies demonstrating that BAD phosphorylation is reduced due to CuB administration.

The ERK pathway is associated with events involved in tumor development, such as differentiation, cell cycle changes, proliferation, and survival.[40] However, various studies have shown that CuB-mediated ERK1/2 phosphorylation has different effects depending on the cell type.[6] Although the ERK pathway is known to stimulate cell survival and cell proliferation, it may have an apoptotic activating effect under certain conditions.[41] Chan *et al.*[40] and Liu *et al.*[41] showed that CuB increased ERK phosphorylation, whereas Zhang *et al.*[11] and El-Senduny *et al.*[6] showed that CuB decreased ERK phosphorylation. According to our results, Cis did not affect ERK1/2 phosphorylation, and CuB significantly reduced ERK phosphorylation. The greatest reduction was in the combined group due to the effects of CuB. Our results were consistent with the studies of Zhang *et al.*[11] and El-Senduny *et al.*[6]

Raf-1 is one of three isoforms of the Raf family protein kinases that mediates the transport of extracellular signals from receptor tyrosine kinases to the nucleus. Raf-1 activation affects cellular events such as cell proliferation, survival, and apoptosis.[42] In our study, activation of Raf-1 and ERK1/2 was inhibited in CuB-treated cells. In other words, CuB reduced the phosphorylation of Raf-1. Our results are consistent with those of Chan KT *et al.*[40]

In some cancer cells, CuB increased p27 expression.[43,44] Cyclin-dependent kinase inhibitor p27 is an essential regulatory protein involved in regulating the cell cycle. p27 arrests the cell cycle in the G1 phase by inhibiting the cyclin-CDK complex.[43,45] With the phosphorylation at the 198-Thr site, p27 is transported from the nucleus to the cytoplasm in the G1 phase and degraded by the

proteasome pathway. p27 degradation triggers the progression of the cell cycle. This causes the tumor suppressor p27 to gain oncogenic properties.[45,46] In previous studies, CuB increased p27 expression and arrested the cycle in cancer cells at the G1 stage.[43,44] However, p27 phosphorylation was not evaluated in these studies. In our study, we primarily showed that CuB significantly decreased p27 phosphorylation.

PRAS40 is a component of mTORC1 and is responsible for mTOR activation.[47] Increased PRAS40 phosphorylation has been associated with many cancers.[48,49] AKT phosphorylates PRAS40 and reduces its inhibitory effect on mTOR.[47] Khan *et al.*[37] showed that PRAS40 phosphorylation was reduced in non-small cell lung cancer cells treated with CuB. In accordance with this result, we found that CuB reduced the phosphorylation level of PRAS40 by half compared to the control group.

Shang *et al.*[44] reported that CuB treatment inhibited the AKT pathway by increasing the tumor suppressor PTEN. Niu *et al.*[16] found that CuB increased PTEN phosphorylation in BEL-7402 cells. However, we did not find any significant differences in the levels of PTEN phosphorylation between the treatment groups and the control group. Surprisingly, the levels of phosphorylated 4E-BP1, GSK3a, GSK3b, P53, P70S6K, PDK1, RPS6, RSK1, and RSK2 were not significantly changed in any of the treated groups, suggesting that those genes may not be upstream targets of CuB and Cis.

Increases in tumor volume were significantly suppressed in an MB49 bladder syngeneic mouse model treated with Cis-alone, CuB-alone, or combined CuB + Cis at weeks 1–3 (experiment termination) compared to untreated controls. Tumor volume measurements were highly correlated with tumor weight. The group with the highest decrease in tumor volume and weight was the combined treatment group; this was due to CuB. The smallest degree of tumor development was observed during the CuB + Cis treatment, whereas the largest tumor diameter and the largest necrosis area were observed in the control group. The combination of CuB and Cis may be an innovation that not only decreases the toxicity of Cis but also increases the anti-tumor effects of Cis. These promising results prompted us to evaluate the possibility of using CuB to treat bladder cancer—either alone or in combination with current chemotherapeutic agents such as Cis—to improve the response rates and reduce toxicity.

Conclusion

This is the first study to demonstrate that CuB alone and combined with Cis significantly reduces tumor growth through caspase-dependent/independent apoptotic and autophagic pathways in bladder cancer tumor tissues. Our results will have major implications for further clinical investigations and the development of new treatment methods that can support conventional treatments for bladder cancer. Future studies should investigate the molecular pathways targeted by CuB for the treatment of bladder cancer.

Authors' contributions: YK and EK conceived and designed the research; YK and IK performed the experiments; AUD participated in the analysis of the data; GE performed histological analysis; EK, CYB and SS interpreted the data; YK and EK wrote the manuscript. The paper was approved by all authors.

DECLARATION OF CONFLICTING INTERESTS

The author(s) declared no potential conflicts of interest with respect to the research, authorship, and/or publication of this article.

FUNDING

This study was conducted with financial support from the Gazi University Research Fund [the project code number 01/2018–28]; and by the Faculty Member Training Program (ÖYP) of the Council of Higher Education of Turkey (YÖK).

ORCID iD

Ece Konac https://orcid.org/0000-0001-5129-2515

REFERENCES

1. Bray F, Ferlay J, Soerjomataram I, Siegel RL, Torre LA, Jemal A. Global cancer statistics 2018: GLOBOCAN estimates of incidence and mortality worldwide for 36 cancers in 185 countries. *CA Cancer J Clin* 2018;**68**:394–424
2. Massari F, Santoni M, Ciccarese C, Brunelli M, Conti A, Santini D, Montironi R, Cascinu S, Tortora G. Emerging concepts on drug resistance in bladder cancer: ımplications for future strategies. *Crit Rev Oncol Hematol* 2015;**96**:81–90
3. Dai G, Yu L, Yang J, Xia K, Zhang Z, Liu G, Gao T, Guo W. The synergistic antitumor effect of cinobufagin and cisplatin in human osteosarcoma cell line in vitro and in vivo. *Oncotarget* 2017;**8**:85150–68
4. Ma X, Dang C, Kang H, Dai Z, Lin S, Guan H, Liu X, Wang X, Hui W. Saikosaponin-D reduces cisplatin-induced nephrotoxicity by repressing ROS-mediated activation of MAPK and NF-κB signalling pathways. *Int Immunopharmacol* 2015;**28**:399–408
5. Liu T, Peng H, Zhang M, Deng Y, Wu Z. Cucurbitacin B, a small molecule inhibitor of the Stat3 signaling pathway, enhances the chemosensitivity of laryngeal squamous cell carcinoma cells to cisplatin. *Eur J Pharmacol* 2010;**641**:15–22
6. El-Senduny FF, Badria FA, El-Waseef AM, Chauhan SC, Halaweish F. Approach for chemosensitization of cisplatin-resistant ovarian cancer by cucurbitacin B. *Tumour Biol* 2016;**37**:685–98
7. Chen W, Leiter A, Yin D, Meiring M, Louw VJ, Koeffler HP. Cucurbitacin B inhibits growth, arrests the cell cycle, and potentiates antiproliferative efficacy of cisplatin in cutaneous squamous cell carcinoma cell lines. *Int J Oncol* 2010;**37**:737–43
8. Qin S, Li J, Si Y, He Z, Zhang T, Wang D, Liu X, Guo Y, Zhang L, Li S, Li Q, Liu Y. Cucurbitacin B induces inhibitory effects via CIP2A/PP2A/Akt pathway in glioblastoma multiforme. *Mol Carcinog* 2018;**57**:687–99
9. Chan KT, Meng FY, Li Q, Ho CY, Lam TS, To Y, Lee WH, Li M, Chu KH, Toh M. Cucurbitacin B induces apoptosis and S phase cell cycle arrest in BEL-7402 human hepatocellular carcinoma cells and is effective via oral administration. *Cancer Lett* 2010;**294**:118–24
10. Zhu JS, Ouyang DY, Shi ZJ, Xu LH, Zhang YT, He XH. Cucurbitacin B induces cell cycle arrest, apoptosis and autophagy associated with G actin reduction and persistent activation of cofilin in Jurkat cells. *Pharmacology* 2012;**89**:348–56
11. Zhang ZR, Gao MX, Yang K. Cucurbitacin B inhibits cell proliferation and induces apoptosis in human osteosarcoma cells via modulation of the JAK2/STAT3 and MAPK pathways. *Exp Ther Med* 2017;**14**:805–12

12. Liu P, Xiang Y, Liu X, Zhang T, Yang R, Chen S, Xu L, Yu Zhao H, Zhang L, Liu Y, Si Y. Cucurbitacin B ınduces the lysosomal degradation of EGFR and suppresses the CIP2A/PP2A/Akt signaling axis in gefitinib-resistant non-small cell lung cancer. *Molecules* 2019;**24**:E647
13. Ding X, Chi J, Yang X, Hao J, Liu C, Zhu C, Wang X, Liu X, Niu Y, Ji W, Chen D, Wu X. Cucurbitacin B synergistically enhances the apoptosis-inducing effect of arsenic trioxide by inhibiting STAT3 phosphorylation in lymphoma Ramos cells. *Leuk Lymphoma* 2017;**58**:2439–51
14. Zhang T, Li Y, Park KA, Byun HS, Won M, Jeon J, Lee Y, Seok JH, Choi SW, Lee SH, Man Kim J, Lee JH, Son CG, Lee ZW, Shen HM, Hur GM. Cucurbitacin induces autophagy through mitochondrial ROS production which counteracts to limit caspase-dependent apoptosis. *Autophagy* 2012;**8**:559–76
15. Ren G, Sha T, Guo J, Li W, Lu J, Chen X. Cucurbitacin B induces DNA damage and autophagy mediated by reactive oxygen species (ROS) in MCF-7 breast cancer cells. *J Nat Med* 2015;**69**:522–30
16. Niu Y, Sun W, Lu JJ, Ma DL, Leung CH1, Pei L, Chen X. PTEN activation by DNA damage ınduces protective autophagy in response to cucurbitacin B in hepatocellular carcinoma cells. *Oxid Med Cell Longev* 2016;**2016**:4313204
17. Liu X, Duan C, Ji J, Zhang T, Yuan X, Zhang Y, Ma W, Yang J, Yang L, Jiang Z, Yu H, Liu Y. Cucurbitacin B induces autophagy and apoptosis by suppressing CIP2A/PP2A/mTORC1 signaling axis in human cisplatin resistant gastric cancer cells. *Oncol Rep* 2017;**38**:271–8
18. Ding Q, Bao J, Zhao W, Hu Y, Lu J, Chen X. Natural autophagy regulators in cancer therapy: a review. *Phytochem Rev* 2015;**14**:137–54
19. Ávalos Y, Canales J, Bravo-Sagua R, Criollo A, Lavandero S, Quest AF. Tumor suppression and promotion by autophagy. *Biomed Res Int* 2014;**2014**:603980
20. Aribi A, Gery S, Lee DH, Thoennissen NH, Thoennissen GB, Alvarez R, Ho Q, Lee K, Doan NB, Chan KT, Toh M, Said JW, Koeffler HP. The triterpenoid cucurbitacin B augments the antiproliferative activity of chemotherapy in human breast cancer. *Int J Cancer* 2013;**132**:2730–7
21. Oberoi HS, Nukolova NV, Laquer FC, Poluektova LY, Huang J, Alnouti Y, Yokohira M, Arnold LL, Kabanov AV, Cohen SM, Bronich TK. Cisplatin-loaded core cross-linked micelles: comparative pharmacokinetics, antitumor activity, and toxicity in mice. *Int J Nanomedicine* 2012;**7**:2557–71
22. Guindon J, Deng L, Fan B, Wager-Miller J, Hohmann AG. Optimization of a cisplatin model of chemotherapy-induced peripheral neuropathy in mice: use of vitamin C and sodium bicarbonate pretreatments to reduce nephrotoxicity and improve animal health status. *Mol Pain* 2014;**10**:56
23. Mani J, Vallo S, Rakel S, Antonietti P, Gessler F, Blaheta R, Bartsch G, Michaelis M, Cinatl J, Haferkamp A, Kögel D. Chemoresistance is associated with increased cytoprotective autophagy and diminished apoptosis in bladder cancer cells treated with the BH3 mimetic (-)-Gossypol (AT-101). *BMC Cancer* 2015;**15**:224
24. Constantinou C, Papas KA, Constantinou AI. Caspase-independent pathways of programmed cell death: the unraveling of new targets of cancer therapy? *Curr Cancer Drug Targets* 2009;**9**:717–28
25. Sun YS, Lv LX, Zhao Z, He X, You L, Liu JK, Li YQ. Cordycepol C induces caspase-independent apoptosis in human hepatocellular carcinoma HepG2 cells. *Biol Pharm Bull* 2014;**37**:608–17
26. Sun J, Feng Y, Wang Y, Ji Q, Cai G, Shi L, Wang Y, Huang Y, Zhang J, Li Q. α-hederin induces autophagic cell death in colorectal cancer cells through reactive oxygen species dependent AMPK/mTOR signaling pathway activation. *Int J Oncol* 2019;**54**:1601–12
27. Kabeya Y, Mizushima N, Ueno T, Yamamoto A, Kirisako T, Noda T, Kominami E, Ohsumi Y, Yoshimori T. LC3, a mammalian homologue of yeast Apg8p, is localized in autophagosome membranes after processing. *Embo J* 2000;**19**:5720–8
28. Qian HR, Yang Y. Functional role of autophagy in gastric cancer. *Oncotarget* 2016;**7**:17641–51
29. Sun L, Liu N, Liu SS, Xia WY, Liu MY, Li LF, Gao JX. Beclin-1-independent autophagy mediates programmed cancer cell death through interplays with endoplasmic reticulum and/or mitochondria in colbat chloride-induced hypoxia. *Am J Cancer Res* 2015;**5**:2626–42
30. Athamneh K, Hasasna HE, Samri HA, Attoub S, Arafat K, Benhalilou N, Rashedi AA, Dhaheri YA, AbuQamar S, Eid A, Iratni R. Rhus coriaria increases protein ubiquitination, proteasomal degradation and triggers non-canonical Beclin-1-independent autophagy and apoptotic cell death in colon cancer cells. *Sci Rep* 2017;**7**:11633
31. Kalai Selvi S, Vinoth A, Varadharajan T, Weng CF. Vijaya padma V. Neferine augments therapeutic efficacy of cisplatin through ROS-mediated non-canonical autophagy in human lung adenocarcinoma (A549 cells). *Food Chem Toxicol* 2017;**103**:28–40
32. Hill SM, Wrobel L, Rubinsztein DC. Post-translational modifications of Beclin 1 provide multiple strategies for autophagy regulation. *Cell Death Differ* 2019;**26**:617–29
33. Kim MJ, Hwang GY, Cho MJ, Chi BH, Park SI, Chang IH, Whang YM. Depletion of NBR1 in urothelial carcinoma cells enhances rapamycin-induced apoptosis through impaired autophagy and mitochondrial dysfunction. *J Cell Biochem* 2019;**120**:19186–201
34. Fang CY, Chen JS, Chang SK, Shen CH. Reversine induces autophagic cell death through the AMP-activated protein kinase pathway in urothelial carcinoma cells. *Anticancer Drugs* 2018;**29**:29–39
35. Liu ST, Hui G, Mathis C, Chamie K, Pantuck AJ, Drakaki A. The current status and future role of the phosphoinositide 3 kinase/AKT signaling pathway in urothelial cancer: an old pathway in the new ımmunotherapy era. *Clin Genitourin Cancer* 2018;**16**:e269–e276
36. Li JR, Cheng CL, Yang CR, Ou YC, Wu MJ, Ko JL. Dual inhibitor of phosphoinositide 3-kinase/mammalian target of rapamycin NVP-BEZ235 effectively inhibits cisplatin-resistant urothelial cancer cell growth through autophagic flux. *Toxicol Lett* 2013;**220**:267–76
37. Khan N, Jajeh F, Khan MI, Mukhtar E, Shabana SM1, Mukhtar H. Sestrin-3 modulation is essential for therapeutic efficacy of cucurbitacin B in lung cancer cells. *Carcinogenesis* 2017;**38**:184–95
38. Stickles XB, Marchion DC, Bicaku E, Al Sawah E, Abbasi F, Xiong Y, Bou Zgheib N, Boac BM, Orr BC, Judson PL, Berry A, Hakam A, Wenham RM, Apte SM, Berglund AE, Lancaster JM. BAD-mediated apoptotic pathway is associated with human cancer development. *Int J Mol Med* 2015;**35**:1081–7
39. Youle RJ, Strasser A. The BCL-2 protein family: opposing activities that mediate cell death. *Nat Rev Mol Cell Biol* 2008;**9**:47–59
40. Chan KT, Li K, Liu SL, Chu KH, Toh M, Xie WD. Cucurbitacin B inhibits STAT3 and the Raf/MEK/ERK pathway in leukemia cell line K562. *Cancer Lett* 2010;**289**:46–52
41. Liu T, Zhang M, Zhang H, Sun C, Yang X, Deng Y, Ji W. Combined antitumor activity of cucurbitacin B and docetaxel in laryngeal cancer. *Eur J Pharmacol* 2008;**587**:78–84
42. Cseh B, Doma E, Baccarini M. RAF" neighborhood: protein-protein interaction in the Raf/Mek/Erk pathway. *FEBS Lett* 2014;**588**:2398–406
43. Xie YL, Tao WH2, Yang TX, Qiao JG. Anticancer effect of cucurbitacin B on MKN-45 cells via inhibition of the JAK2/STAT3 signaling pathway. *Exp Ther Med* 2016;**12**:2709–15
44. Shang Y, Guo XX, Li WW, Rao W, Chen ML, Mu LN, Li SJ. Cucurbitacin-B inhibits neuroblastoma cell proliferation through up-regulation of PTEN. *Eur Rev Med Pharmacol Sci* 2014;**18**:3297–303
45. Sun C, Wang G, Wrighton KH, Lin H, Songyang Z, Feng XH, Lin X. Regulation of p27Kip1 phosphorylation and G1 cell cycle progression by protein phosphatase PPM1G. *Am J Cancer Res* 2016;**6**:2207–20
46. Yoon H, Kim M, Jang K, Shin M, Besser A, Xiao X, Zhao D, Wander SA, Briegel K, Morey L, Minn A, Slingerland JM. p27 transcriptionally coregulates cJun to drive programs of tumor progression. *Proc Natl Acad Sci USA U S A* 2019;**116**:7005–14
47. Lv D, Guo L, Zhang T, Huang L. PRAS40 signaling in tumor. *Oncotarget* 2017;**8**:69076–85
48. Madhunapantula SV, Sharma A, Robertson GP. PRAS40 deregulates apoptosis in malignant melanoma. *Cancer Res* 2007;**67**:3626–36
49. Lu YZ, Deng AM, Li LH, Liu GY, Wu GY. Prognostic role of phospho-PRAS40 (Thr246) expression in gastric cancer. *Arch Med Sci* 2014;**10**:149–53

(Received February 21, 2020, Accepted March 17, 2020)